Valence band structures of titanium nitride and titanium carbide calculated with chemically complete clusters

1998 J. Phys.: Condens. Matter 10 9443

(http://iopscience.iop.org/0953-8984/10/42/010)

J. Phys.: Condens. Matter **10** (1998) 9443–9454. Printed in the UK PII: S0953-8984(98)93707-9

Valence band structures of titanium nitride and titanium carbide calculated with chemically complete clusters

Bin Song†, Hirohide Nakamatsu‡, Rika Sekine§, Takeshi Mukoyama‡ and Kazuo Taniguchi†

† Division of Electronics and Applied Physics, Osaka Electro-Communication University, 18-8, Hatsu-machi, Neyagawa, Osaka 572-8530, Japan

‡ Institute for Chemical Research, Kyoto University, Uji, Kyoto 611-0011, Japan

§ Department of Chemistry, Shizuoka University, Ohya 836, Shizuoka 422-8529, Japan

Received 28 April 1998

Abstract. Valence band structures of TiN and TiC have been calculated by the DV-X_α cluster method. A chemically complete cluster $TiX_6Ti_{12}Ti_6$ (X = N or C) is used to improve termination of the cluster and electroneutrality of the Ti–N and Ti–C stoichiometric pairs. Density of states for the valence band, theoretical Ti L_3, Ti K and X K x-ray emission spectra for TiN and TiC are presented and are in good agreement with the experimental ones. Interaction between the metal and non-metal atoms is discussed. Experimental Ti L_3 x-ray emission spectra for TiN and TiC have also been obtained in the present work, using monochromatized synchrotron radiation.

1. Introduction

Titanium nitride (TiN) and carbide (TiC), classified as refractory metal compounds, possess an unusual combination of physical properties [1]. Both TiN and TiC are extremely hard, have very high melting points and exhibit metallic-like electronic conductivity. These properties make them attractive both fundamentally [2] and technologically [3], and are closely connected with their electronic structure. Therefore, these compounds arouse theoretical [4–19] and experimental [19–29] interest, specially for their valence band structures.

From an experimental standpoint, x-ray spectroscopy is one of the most powerful tools for elucidating electronic structures of substances [30, 31]. Valence band structure can be studied with x-ray photoelectron spectra (XPS) and x-ray emission spectra (XES). XPS reflects density of states (DOS), while XES reflects partial density of states (PDOS). Detailed information on band structures and chemical bonding can be obtained by combining XPS and XES. According to the dipole selection rule on the phototransition, the K emission band reflects p components and the L_3 emission band corresponds to s and d components. Therefore, detailed valence band structures for TiN and TiC will be clarified by combining the valence band XPS, Ti, L_3 XES and Ti Kβ_5, non-metal (C or N) Kα spectra.

Many researchers studied the valence band structures of TiN and TiC by XES [19–24] or XPS [25–29]. It is difficult to reduce electronic structures from $L_{2,3}$ emission spectra because of the self-absorption and the Coster–Kronig transitions. Recently, the synchrotron radiation technique has allowed selection of the excitation energy for the photon-excited emission spectroscopy. This makes it possible to obtain metal L_3 XES for TiN, $CaSi_2$, CaSi and TiO_2, getting rid of the obstacles mentioned above [20, 31, 32]. However, to our

0953-8984/98/429443+12$19.50

knowledge, the Ti L_3 XES of TiC excited by the synchrotron radiation has not been reported yet.

On the other hand, the valence band structures of TiN and TiC have been calculated by various band [4–12] and cluster [13–16] methods. Augmented-plane-wave (APW) band calculations were performed by several researchers [4–7]. These APW calculations have not given equivalent results with each other. APW calculations with the LCAO interpolation scheme done by Neckel *et al* [7] are evaluated highly in the early works [4–6] because most of the subsequent experimental works [27–29] showed that their results were comparable with Neckel's. Recently, the mixed-basis band structure interpolation scheme (MBBSIS) [8], the full-potential linear muffin-tin orbital (LMTO) [9, 10] and the charge-self-consistent LCAO [11] band calculations have been reported. Nevertheless, discrepancies between the recent results of the band calculations still exist. There are remarkable differences between them in shape of the DOS and quantity of charge transfer between the constituent atoms.

Compared with the band calculations, cluster calculations of TiN or TiC are relatively scarce. Gubanov *et al* [13] have performed MS-X_α calculations on TiC, using a TiC_6^{20-} cluster. Their theoretical XPS of the valence band was compared with a low-resolution spectrum. However, their result has appreciable differences from the later experimental photoelectron spectrum with high resolution [29]. Lowther [14] carried out CNDO/2 calculations on TiC with the molecular orbital scheme, but the density of states disagreed with the experimental photoelectron spectrum [29].

Up to the present, most of the valence band structure calculations for TiN and TiC compared only the DOS with the experimental photoelectron spectra of the valence band. XES for these compounds have been discussed with cluster calculations though the theoretical spectra were not satisfactory [15–17]. The simplest TiX_6^{n-} (X = C or N) model cluster is still used to interpret the origins of the peaks in the XES. Weinberger [17] interpreted the Ti L_3, Ti K and non-metal K XES of these compounds with SW-X_α calculations. But in the Ti L_3 spectrum for TiN, the ratio of the calculated peak intensities was significantly different from that of the experimental ones. His theoretical spectra could not explain bands at the highest energy in the N Kα and Ti Kβ_5 spectra. Gubanov *et al* [16] reported the same discrepancy of the uppermost bands for TiN and they explained that it could be due to defect structures in the crystal. Weinberger has suggested that the cluster TiX_6^{n-} he used might be the origin of discrepancies and larger clusters $TiX_6Ti_m^{n-}$ would be necessary to clear up the above discrepancies. We consider that some points inherent in the crystals are missing in the simple TiX_6^{n-} cluster. The TiX_6^{n-} cluster has a sudden change of bonding environment at the periphery. It causes peculiar charge distribution different from the actual crystal. Moreover, electroneutrality for the Ti–X pair is not achieved in the cluster. Earlier than the cluster calculations mentioned above, Neckel *et al* [18] gave the local partial DOS histograms to interpret the XES of the same compounds, using APW band calculations. The uppermost band is seen in the N Kα spectra, but it is indistinguishably small in the Ti Kβ_5 spectra for TiN.

In the present work, in order to provide theoretical spectra of high quality, chemically complete clusters are employed. These clusters improve the periphery of clusters and the electroneutrality in the stoichiometric composition of crystals. Furthermore, in order to make a precise comparison with experimental spectra, Ti L_3 XES for TiN and TiC are measured, using synchrotron radiation. We will show that the present calculations are in good agreement with the experimental photoelectron spectra and XES. This agreement encourages us to discuss valence band electronic structures of TiN and TiC and to compare the covalency of the compounds. In section 2, essential points of the Ti L_3 XES measurement of TiN and TiC will be given. In section 3, the calculation method and the chemically

complete cluster model will be described. In section 4, comparison of the theoretical spectra with the experimental ones will be carried out. The total DOS and partial DOSs projected onto the different atomic components will be presented and the electronic structures will be discussed.

2. Experiment

The Ti L_3 XES for TiN and TiC were obtained at the undulator beamline 8.0 [33] of the Advanced Light Source in Lawrence Berkeley Laboratory. Emitted photons were detected at a high-efficiency fluorescence endstation [33] consisting of an ultrahigh vacuum sample chamber and a grazing incidence concave grating spectrometer which had a fixed entrance slit and a position sensitive area detector. An entrance slit of 100 μm and a ruling of 600 lines mm^{-1}, 10 m radius grating were used for the present measurement. The excitation energy for Ti L_3 XES was changed from 456 eV to 459 eV with a step of 1.0 eV for both TiN and TiC. The difference between the spectra obtained with this range of the excitation energy was not appreciable. The specimens were commercially available TiN and TiC (Soekawa Chemical Co.) with the minimum purity of 99%.

3. Computational method

Computational details of the SCAT code used in the present work to execute the DV-X_α molecular orbital calculations have been described in [34]. The DV-X_α method is outlined in the following.

The exchange potential is described as

$$V_x(r) = -3\alpha[(3/8\pi)\rho(r)]^{1/3} \tag{1}$$

where ρ is the electron density and α is the Slater exchange parameter. The matrix elements in the secular equation are derived from a weighted sum of integrand values at sample points [35]. Therefore, difficulties of analytical multicentre integrations are avoided with this numerical integration procedure. The potential was produced by the sum of contributions from atomic orbitals. It is more realistic than the muffin-tin potential used in most of the band calculations. In the SCAT code used, atomic orbitals were numerical solutions for an atomic-like potential and obtained at an initial stage of each iteration for the self-consistent procedures.

A chemically complete cluster method has been proposed in [36]. In the present work, a variant with some different points [37, 38] was implemented. A diagram for the chemically complete cluster is shown in figure 1. The central atoms were chemically complete atoms. The neighbouring atoms had the potentials duplicated from those of the corresponding central atoms. As a result of the duplication of the potentials and the self-consistent procedures, the central atoms were put into an equivalent for the environment in the crystal. This cluster consisting of the chemically complete atoms and the neighbouring atoms was embedded in surrounding potentials which were duplicated from the potentials of the central atoms. Pseudopotentials were placed upon these potentials so that the wave functions of the embedded cluster feel the exclusive character of the wave functions of the surrounding atoms. The electroneutrality of the Ti–X stoichiometric pair was achieved by varying the depth of the pseudopotentials. This procedure was taken to compensate for the change of the chemical potential of electrons at the ends of the embedded cluster. Electrostatic potential due to ions in a compound is calculated with direct summation of the Coulomb

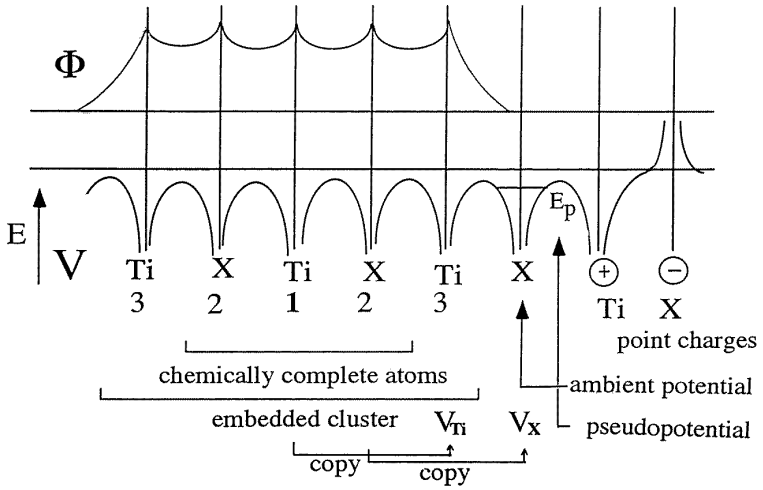

Figure 1. Diagram for chemically complete cluster model.

potential of point charges by the Coker method [39, 40] though the electrostatic potential was unnecessary for the present metallic compounds.

The model cluster $TiX_6Ti_{12}Ti_6$ for TiN and TiC used in the present calculations is shown in figure 2. The atom at the centre was a Ti atom and the cluster was extended to the second and third nearest neighbour Ti atoms, $Ti_{12}Ti_6$, so that the X_6 atoms were thoroughly surrounded by the nearest neighbour Ti atoms. This cluster with O_h symmetry was embedded in 56 surrounding potentials of the X atoms. Atomic orbitals of Ti 1s–4p and X 1s–2p were used as the basis functions. The TiX has the rock salt structure. The Ti–N and Ti–C distances were taken to be 2.1175 and 2.1593 Å, respectively [41]. In all the calculations, the Slater exchange parameter was chosen to be 0.7 [34].

X-ray emission probability I_j in the dipole approximation is written as [42]

$$I_j \propto E_j^3 D_j^2 \tag{2}$$

where E_j is the transition energy of an electron from the jth MO to the hole in the inner shell and D_j is the dipole matrix element:

$$D_j = \langle \varphi_h | \boldsymbol{r} | \varphi_j \rangle \tag{3}$$

where φ_h is the wave function of the inner shell hole, $\boldsymbol{r}$ is the position vector and φ_j is the wave function of the jth MO. In the present work, the emission intensity was estimated with a software called SXS [43] with improved precision of integration [44]. The wave functions in the ground state were used. Intensities for three kinds of Ti atom in the cluster were summed up to evaluate all the forms of the wavefunctions in the cluster. This summation corresponds to collecting all the momenta of the wavefunctions. To generate the theoretical spectra, a Lorentzian curve was placed at each eigenenergy. Its height was proportional to the intensity and its width was 3.0 eV (FWHM) for all the present XES. The DOS was derived from the MO levels replaced with Lorentzian curves with the peak width (FWHM) of 1.0 eV.

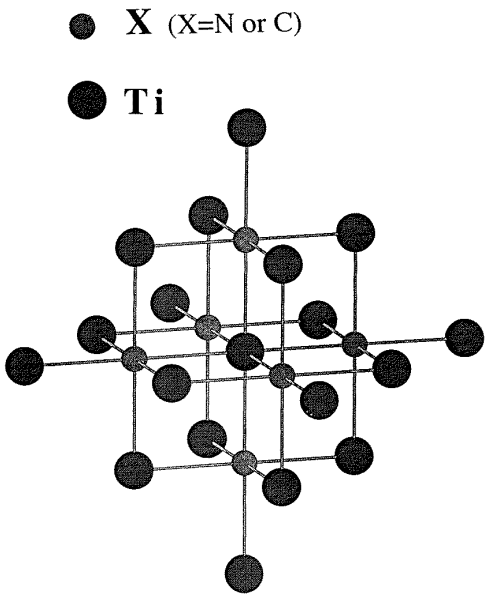

Figure 2. $TiX_6Ti_{12}Ti_6$ cluster for TiX (X = N or C).

4. Results and discussion

4.1. Valence band XPS and XES

The theoretical DOS and XES obtained are compared with the experimental spectra and the relation among the spectra is illustrated in the present section. The theoretical valence DOS and XES for TiN are plotted in figure 3 and the experimental spectra are in figure 4. The spectra for TiC are in figures 5 and 6. The theoretical spectra are arranged according to the energy of the ground state.

As stated in section 3, the chemically complete cluster $TiX_6Ti_{12}Ti_6$ (X = C or N) was used to calculate the valence band structures for stoichiometric TiN and TiC. The crystallographically equivalent sites and the electroneutrality are taken into consideration to obtain the crystal environment, which is achieved with the chemically complete clusters. However, the cluster $TiX_6Ti_{12}Ti_6$ does not have the atomic ratio of TiX. In order to derive the DOS for TiX, we used the components for the TiX_6Ti_4Ti composition instead of the $TiX_6Ti_{12}Ti_6$ cluster. The components of the second and third Ti atoms in the $TiX_6Ti_{12}Ti_6$ cluster are divided by three and six, respectively, to derive the TiX_6Ti_4Ti composition. These dividing factors come from the number of nearest atoms neighbouring the second and third Ti atoms in the cluster. The second and third Ti atoms have only two and one adjacent X atoms, respectively, though the atoms in the crystal have six neighbours. This is only one of the ways to obtain the stoichiometric composition from the cluster and was found to be satisfactory for the present discussion. The components of the chemically incomplete part Ti_4Ti were corrected on the basis of the component ratio among Ti 3d, X 2s and 2p for the chemically complete TiX atoms.

For comparison, the experimental valence photoelectron spectra [29] with the excitation energy 190 eV and Ti L_3, Ti K and non-metal K XES [17] for TiN and TiC are shown in figures 4 and 6, respectively. The Ti L_3 XES for TiN and TiC were measured in the present

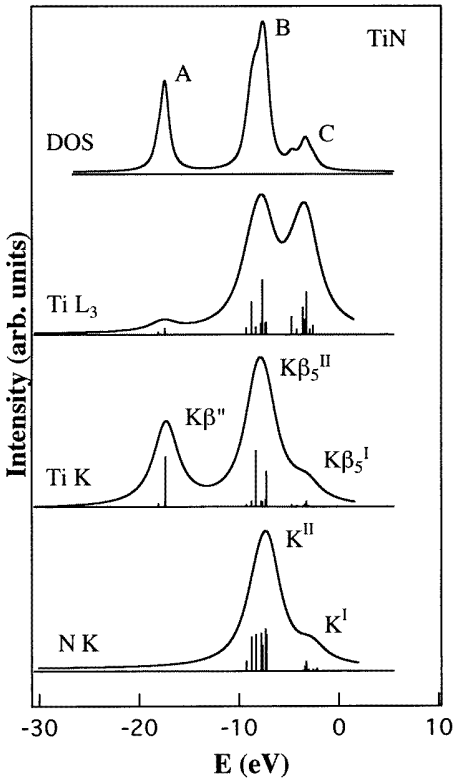

Figure 3. Theoretical DOS and XES for TiN. Theoretical Ti L_3, Ti K and N K are aligned with a energy scale of the ground state.

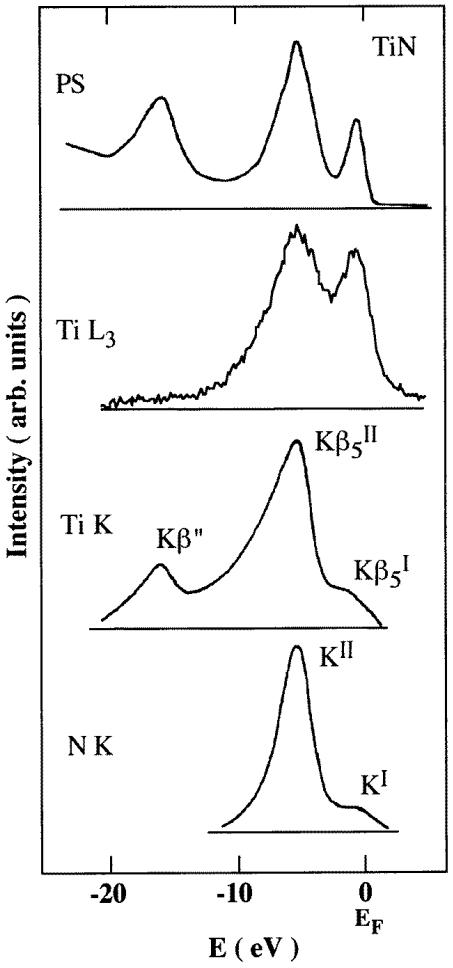

Figure 4. Experimental photoelectron spectra [29], Ti L_3, Ti K and N K XES [17] for TiN. See the text for the energy alignment of the different spectra.

work for the excitation energies of 458 and 456 eV, respectively. These excitation energies are lower than the $2p_{1/2}$ ionization energy for TiN and TiC so that they give the clear Ti L_3 spectra which result from the transition from the valence band to the $2p_{3/2}$ hole of the Ti atoms. Although the measured Ti L_3 XES for TiN is quite similar to that measured by Rubensson *et al* [20], there is a difference in the peak intensity at the highest energy. This peak in the present Ti L_3 emission spectrum is slightly higher than that of Rubensson.

The Ti L_3, Ti K and non-metal K spectra were arranged, referring to the Ti $2p_{3/2}$, Ti 1s and non-metal 1s ionization energies for TiN and TiC [26, 45, 46]. The x-ray emission energy is expressed as

$$E_{XE} = -\{E(\mathrm{V}^0\mathrm{C}^1) - E(\mathrm{V}^1\mathrm{C}^0)\} \tag{4}$$

where $E(\mathrm{V}^1\mathrm{C}^0)$ is the total energy in the initial state with a hole in an inner-shell level C and $E(\mathrm{V}^0\mathrm{C}^1)$ is the total energy after the electron transition from a valence level V to the

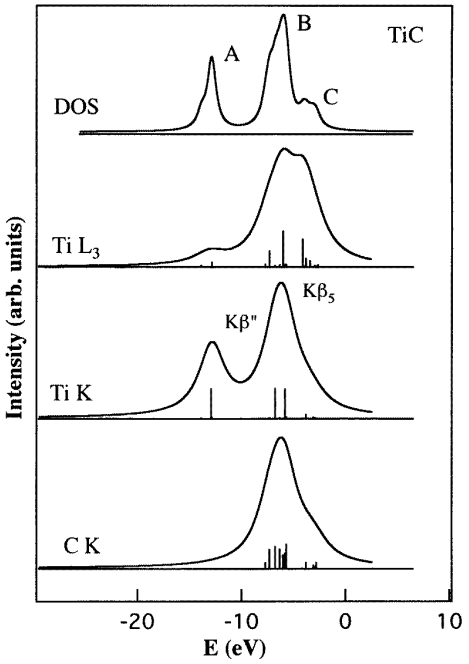

Figure 5. Theoretical DOS and XES for TiC. Theoretical Ti L_3, Ti K and C K are aligned with a energy scale of the ground state.

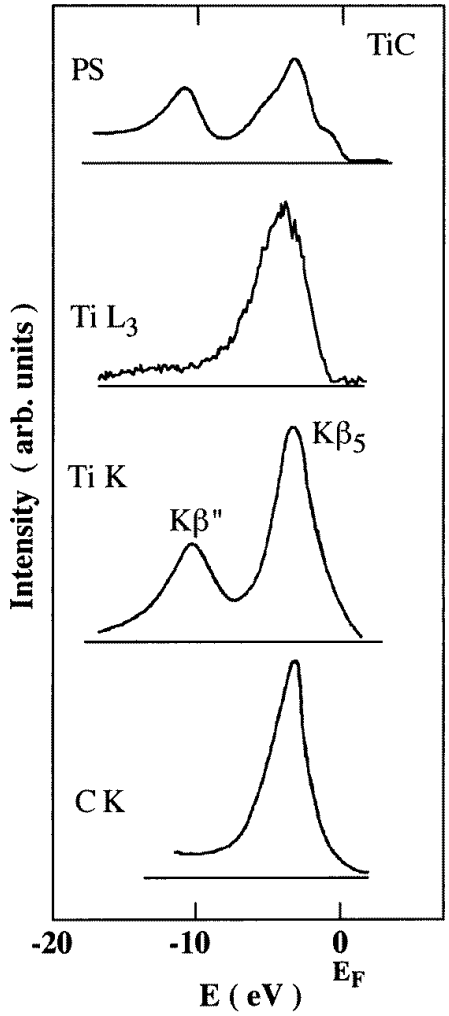

Figure 6. Experimental photoelectron spectra [29], Ti L_3, Ti K and C K XES [17] for TiC. See the text for the energy alignment of the different spectra.

inner-shell C. The ionization energy E_I for the inner-shell level is written as

$$E_I = E(\mathrm{V}^1\mathrm{C}^0) - E(\mathrm{V}^1\mathrm{C}^1) \tag{5}$$

where $E(\mathrm{V}^1\mathrm{C}^1)$ is the energy for the ground state and $E(\mathrm{V}^1\mathrm{C}^0)$ is the energy after the ionization from the inner-shell level C. Therefore, we have

$$E_I - E_{XE} = E(\mathrm{V}^0\mathrm{C}^1) - E(\mathrm{V}^1\mathrm{C}^1). \tag{6}$$

The right-hand side of this equation means the ionization energy for the valence level. Consequently, we arrange the different XES on the basis of equation (6). The origin of the energy is the Fermi energy, which arises from the ionization energy measurement for solids.

The total DOS for TiN (figure 3) shows good agreement with the experimental photoelectron spectrum (figure 4). Neckel's [7] and Ahuja's [10] results are similar to ours. The theoretical results reproduce all the three bands in the experimental spectrum. The energy difference between the band B and band C is in very good agreement with that in the experimental one. Band A is, however, located about 1 eV higher in the theoretical spectrum than observed experimentally. This narrow interval between N 2s and 2p is found even in the atomic calculations with the local density functionals. The height of the band C is larger in the experimental spectrum than in the theoretical one. Photoelectron intensity calculations are necessary to discuss it in detail.

For TiN, the theoretical XES in figure 3 also agree well in shape and position with the experimental spectra of the Ti L_3, Ti K and N K XES shown in figure 4. The present theoretical spectra have the uppermost peaks marked with $K\beta_5^I$ and K^I in the Ti K and N K XES, which could not be explained with the simplest cluster TiX_6^{n-} calculations [16, 17]. The calculated peak intensities for Ti L_3, Ti K and N K are also in good agreement with the corresponding experimental ones.

For TiC, general features and agreement with the experimental spectra are similar to those for TiN. The total DOS, theoretical Ti L_3, Ti K and C K XES were summarized in figure 5, compared with the experimental spectra shown in figure 6. All the features in the experimental spectra are observed in the theoretical ones. In contrast to TiN which shows the separate bands B and C, the two bands of TiC are so close that the highest energy structures in XES are not observed clearly.

Figures 3 to 6 for TiN and TiC also reveal consistency of the peak positions among the spectra. We can make definite conclusions about the peak positions projected onto the different spectra and thus obtain the details of the valence bands of these compounds. The peak positions in the experimental spectra for TiN are consistent with each other in figure 4 and the correlation among the theoretical spectra in figure 3 confirms that among the experimental ones. As for TiC, consistency is obtained except for the experimental Ti L_3 XES shown in figure 6. It resides about 0.5 eV lower than the corresponding peak in the other spectra. This discrepancy can be attributed to a measurement error of the absolute energy in the Ti L_3 XES or the ionization energy.

The present DOS for TiN and TiC are comparable to those of Neckel *et al* [7]. Concerning the XES, the present work has drawn the direct and clear conclusions in respect of the intensity evaluation and the uppermost peaks Ti $K\beta_5^I$ and N K^I. Neckel *et al* showed the partial DOS histograms to interpret the XES [18] and Ti $K\beta_5^I$ was not distinct. Furthermore, in the present work, the clear correlations among the spectra are demonstrated.

4.2. Valence band structure

The DOS and partial DOSs projected onto the orbital components shown in figure 7 give information about the valence band structure of TiN. Three bands symbolized A, B and C are observed in the valence band. The bands B and C are separate subbands but merge with each other. The lowest energy band A is formed mainly from the N 2s states with a little admixture of the Ti states. The next subband B is situated 10 eV above the band A. This subband originates from the main N 2p states and contains also a significant contribution of the Ti 3d states. Finally, the subband C includes mainly the Ti 3d states but exhibits also a small amount of the N 2p states. These descriptions of the valence band structure agree with those of other calculations [7, 10]. The Ti s and p states also contribute to the valence band to a limited extent.

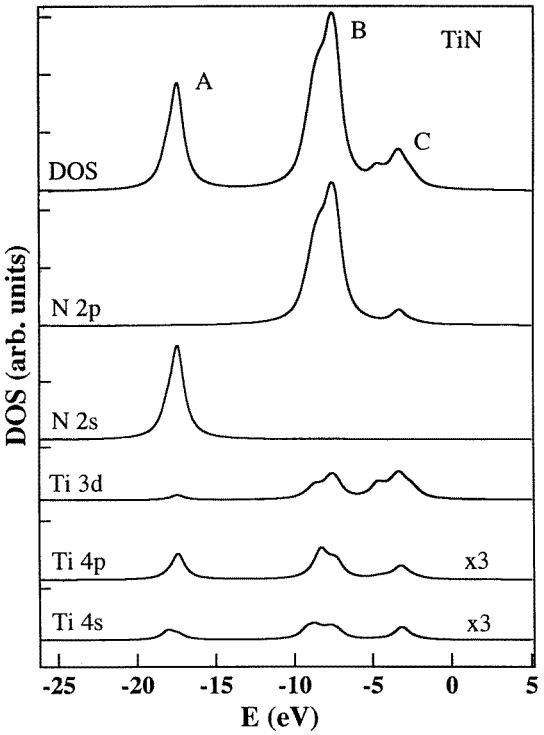

Figure 7. Total and partial DOS for TiN. Each partial DOS is marked with its atomic orbital component.

The total DOS and partial DOSs for TiC are shown in figure 8. These DOSs are similar to that for TiN. This is not surprising when one takes account of the close chemical and structural relation between these compounds. It is a main difference that the bands B and C are closer in TiC than in TiN. This difference is connected with an atomic property. The larger electronegativity of the N atom means a lower 2p level in TiN than in TiC, Therefore, the gap between the non-metal 2p and Ti 3d levels is larger in TiN than in TiC.

In order to discuss covalency of the TiX compounds, the X 2p band is analysed, where the Ti components mean the covalency contributions of Ti. The atomic orbital populations in the valence 2p bands are summarized in table 1. It is clearly observed that the metal components are considerably mixed into the non-metal 2p bands of the TiC and TiN compounds. The Ti 3d states contributing to the valence 2p bands in TiC and TiN are twice as large as those in TiO_2 [47] which is an insulator with an ionic property. In addition, the Ti 4s and 4p states in the valence 2p bands are also much larger due to the metallic property. These Ti 4s and 4p contributions were experimentally revealed by Didziulis *et al* [26], who observed resonant effects in the photoelectron spectroscopy of TiC and TiN and concluded that the participations of the Ti 4s and 4p components were significant in the valence bands. The present results support their conclusion. The comparable amounts of Ti 3d, 4s and 4p to that of non-metal 2p indicate that stronger interaction between the metal and non-metal atoms occurs in TiN and TiC than in TiO_2. This strong interaction may produce the extreme hardness of TiN and TiC.

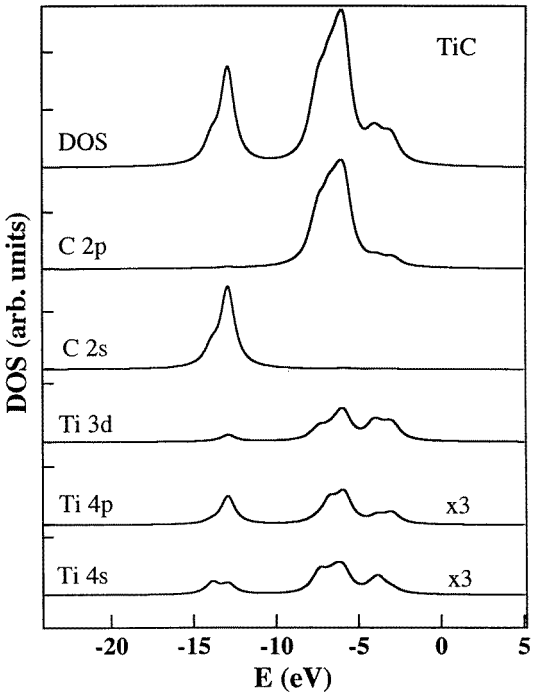

Figure 8. Total and partial DOS for TiC. Each partial DOS is marked with its atomic orbital component.

Table 1. Atomic orbital populations in valence 2p band.

	Metal			Non-metal	
	3d	4s	4p	2s	2p
TiC	1.58	1.00	0.66	0.06	2.70
TiN	1.36	0.64	0.54	0.00	3.44
TiO_2[a]	0.64	−0.12	−0.16	0.00	5.62

[a] Computational features are described in [47].

Table 1 shows that the Ti 3d contribution as well as Ti 4s, 4p decreases in the order of TiC, TiN and TiO_2. This indicates that the covalency due to the interaction between the non-metal and metal atoms decreases in this order. Kim and Williams [8] analysed the DOS and showed that the d-like components in the non-metal 2p band decreased in the order of TiC, TiN and TiO. Performing APW calculations, Blaha and Schwarz [12] compared spatial distributions of the electron density of these compounds and found that the densities around the non-metal atoms became localized in the series of the TiC, TiN and TiO. The present work has clarified the same tendency of the covalency as these earlier results. This tendency is consistent with the above-mentioned wider gap between the Ti 3d and non-metal 2p bands for TiN than for TiC. The present results, however, do not support a conclusion based on x-ray diffraction [48] or analysis of x-ray emission spectra [21], which exhibited the opposite tendency of the covalency of TiN and TiC.

5. Conclusion

In the present work, we have performed the DV-X_α calculations to clarify the valence band structures for TiN and TiC with the chemically complete clusters, which improve the termination of the cluster and the electroneutrality in the TiN and TiC stoichiometric compositions. The density of states for the valence band, theoretical Ti L_3, Ti K and non-metal K XES for TiN and TiC are obtained and are in good agreement with the experimental ones. Both of the theoretical spectra and the aligned experimental ones have consistently revealed the peak correlation among the spectra. The present results have demonstrated the uppermost bands in the N Kα and Ti Kβ_5 spectra for TiN, though the earlier cluster calculations [16, 17] could not derive them and one of them was not clear in the partial DOS with the band calculation [18].

The DOS results reveal strong metal 3d–non-metal 2p interaction in these compounds and this interaction decreases from TiC to TiN. In order to avoid the effects of the self-absorption and the Coster–Kronig transitions of the Ti $L_{2,3}$ XES and make a precise comparison with experimental spectra, experimental Ti L_3 x-ray emission spectra for TiN and TiC are obtained, using monochromatized synchrotron radiation.

Acknowledgments

The authors thank J Tsuji, Y Nakane and Y Tsuji of Osaka Electro-Communication University, and Dr R C C Perera of Lawrence Berkerley Laboratory, for their help toward the XES measurements.

References

[1] Toth L E 1971 *Transition Metal Carbides and Nitrides* (New York: Academic)
[2] Williams W S 1988 *Mater. Sci. Eng.* A **105/106** 1
[3] Sundgren J E and Hentzell H T G 1986 *J. Vac. Sci. Technol.* A **4** 2259
[4] Ern V and Switendick A C 1965 *Phys. Rev.* A **137** A1927
[5] Conklin J B Jr and Silversmith D J 1968 *Int. J. Quantum. Chem.* **25** 243
[6] Ihara H, Kumashiro Y and Itoh A 1975 *Phys. Rev.* B **12** 5465
[7] Neckel A, Rastl P, Eibler R, Weinberger P and Schwarz K 1976 *J. Phys. C: Solid State Phys.* **9** 579
[8] Kim S and Williams R S 1988 *J. Phys. Chem. Solids* **49** 1307
[9] Price D L and Cooper B R 1989 *Phys. Rev.* B **39** 4945
[10] Ahuja R, Eriksson D, Wills J M and Johansson B 1996 *Phys. Rev.* B **53** 3072
[11] Pai V A, Sathe A P and Marathe V R 1990 *J. Phys.: Condens. Matter* **2** 9363
[12] Blaha P and Schwarz K 1983 *Int. J. Quantum. Chem.* **23** 1535
[13] Gubanov V A, Ivanovskii A L, Shveikin G P and Weber J 1979 *Solid State Commun.* **29** 743
[14] Lowther J E 1984 *J. Less-Common Met.* **99** 291
[15] Gubanov V A, Kurmaev E Z and Ellis D E 1981 *J. Phys. C: Solid State Phys.* **14** 5567
[16] Gubanov V A, Kurmaev E Z and Shveikin G P 1977 *J. Phys. Chem. Solids* **38** 201
[17] Weinberger P 1976 *Theor. Chim. Acta* **42** 169
[18] Neckel A, Schwarz K, Eibler R, Rastl P and Weinberger P 1975 *Mikrochim. Acta. Suppl.* **6** 257
[19] Gubanov V A and Connolly J W D 1976 *Chem. Phys. Lett.* **44** 139
[20] Rubensson J E, Wassdahl N, Bray G, Rindstedt J, Nyholm R, Cramm S, Martensson N and Nordgren J 1988 *Phys. Rev. Lett.* **60** 1759
[21] Ramquist L, Ekstig B, Kallne E, Noreland E and Manne R 1969 *J. Phys. Chem. Solids* **30** 1849
[22] Holliday J E 1967 *J. Appl. Phys.* **38** 4720
[23] Fischer D W and Baun W L 1968 *J. Appl. Phys.* **39** 4757
[24] Nemnonov S A and Kolobova K M 1966 *Fiz. Met. Metalloved* **22** 680
[25] Soriano L, Abbate M, Pen H, Prieto P and Sanz J M 1997 *Solid State Commun.* **102** 291
[26] Didziulis S V, Lince J R, Stewart T B and Eklund E A 1994 *Inorg. Chem.* **33** 1979

[27] Weaver J H and Schmidt F A 1980 *Phys. Lett.* **77** A 73
[28] Bringans R D and Höchst H 1984 *Phys. Rev.* B **30** 5416
[29] Johansson L I, Stefan P M, Shek M L and Nørlund Christensen A 1980 *Phys. Rev.* B **22** 1032
[30] Meisel A, Leonhardt G and Szargan R 1989 *X-Ray Spectra and Chemical Binding (Springer Series in Chemical Physics 37)* (Berlin: Springer) pp 228–44
[31] Jia J J, Callcott T A, Asfaw A, Carlisle J A, Terminello L J, Ederer D L, Himpsel F J and Perera R C C 1995 *Phys. Rev.* B **52** 4904
[32] Ederer D L *et al* 1996 *X-Ray and Inner-shell Processes, 17th Int. Conf. (Sept. 1996)* ed R L Johnson, H Schmidt-Böcking and B F Sonntag (Woodbury, NY: AIPP) p 764
[33] Jia J J *et al* 1995 *Rev. Sci. Instrum.* **66** 1394
[34] Adachi H, Tsukada M and Satoko C 1978 *J. Phys. Soc. Japan* **45** 875
[35] Averill F W and Ellis D E 1973 *J. Chem. Phys.* **59** 6412
[36] Goodman G L, Ellis D E, Alp E E and Soderholm L 1989 *J. Chem. Phys.* **91** 2983
[37] Nakamatsu H 1994 *Bull. Soc. Discrete Variational* X_α **7** 21
[38] Sekine R, Miyazaki E, Nakamatsu H, Song B and Mukoyama T to be published
[39] Coker H 1983 *J. Phys. Chem.* **87** 2512
[40] Nakamatsu H and Mukoyama T 1994 *Bull. Inst. Chem. Res. Kyoto Univ.* **72** 345
[41] Wyckoff R W G 1982 *Crystal Structures* 2nd edn, vol 1 (Malabar, FL: Robert E Krieger Publishing) p 90
[42] Bethe H A and Salpeter E E 1957 *Quantum Mechanics of One- and Two-Electron Systems* (Berlin: Springer) pp 246–69
[43] Adachi H and Taniguchi K 1980 *J. Phys. Soc. Japan* **49** 1944
[44] Song B, Nakamatsu H, Shigemi A, Mukoyama T and Taniguchi K 1998 *X-Ray Spectrom.* at press
[45] Ramqvist L, Hamrin, K, Johansson G, Fahlman A and Nordling C 1969 *J. Phys. Chem. Solids* **30** 1835
[46] Ramqvist L, Ekstig B, Källne E, Noreland E and Manne R 1969 *J. Phys. Chem. Solids* **30** 1849
[47] Song B, Nakamatsu H, Mukoyama T and Taniguchi K 1998 *Adv. X-ray Chem. Anal. Japan* **29** 191
[48] Dunand A, Flack H D and Yvon K 1985 *Phys. Rev.* B **51** 2299